Plant Physiology®

The role of light-harvesting complex I in excitation energy transfer from LHCII to photosystem I in Arabidopsis

Christo Schiphorst [1,2] Luuk Achterberg [2] Rodrigo Gómez,[1] Rob Koehorst,[2,3] Roberto Bassi [1] Herbert van Amerongen [2,3] Luca Dall'Osto[1] and Emilie Wientjes [2,*,†]

1 Dipartimento di Biotecnologie, Università di Verona, 37134 Verona, Italy
2 Laboratory of Biophysics, Wageningen University, 6700 ET Wageningen, The Netherlands
3 MicroSpectroscopy Research Facility, Wageningen University, 6700 ET Wageningen, The Netherlands

*Author for correspondence: emilie.wientjes@wur.nl
†Senior author.
E.W., R.G., C.S., L.D.O. designed the research; C.S., L.A., R.G., R.K., performed the research; C.S., L.A., R.G., R.B., H.v.A., L.D.O., E.W. analyzed the data; and C.S., H.v.A., L.D.O., E.W. wrote the paper.
The author responsible for distribution of materials integral to the findings presented in this article in accordance with the policy described in the Instructions for Authors (https://academic.oup.com/plphys/pages/general-instructions) is: E. Wientjes (emilie.wientjes@wur.nl).

Abstract

Photosynthesis powers nearly all life on Earth. Light absorbed by photosystems drives the conversion of water and carbon dioxide into sugars. In plants, photosystem I (PSI) and photosystem II (PSII) work in series to drive the electron transport from water to $NADP^+$. As both photosystems largely work in series, a balanced excitation pressure is required for optimal photosynthetic performance. Both photosystems are composed of a core and light-harvesting complexes (LHCI) for PSI and LHCII for PSII. When the light conditions favor the excitation of one photosystem over the other, a mobile pool of trimeric LHCII moves between both photosystems thus tuning their antenna cross-section in a process called state transitions. When PSII is overexcited multiple LHCIIs can associate with PSI. A trimeric LHCII binds to PSI at the PsaH/L/O site to form a well-characterized PSI–LHCI–LHCII supercomplex. The binding site(s) of the "additional" LHCII is still unclear, although a mediating role for LHCI has been proposed. In this work, we measured the PSI antenna size and trapping kinetics of photosynthetic membranes from Arabidopsis (*Arabidopsis thaliana*) plants. Membranes from wild-type (WT) plants were compared to those of the Δ*Lhca* mutant that completely lacks the LHCI antenna. The results showed that "additional" LHCII complexes can transfer energy directly to the PSI core in the absence of LHCI. However, the transfer is about two times faster and therefore more efficient, when LHCI is present. This suggests LHCI mediates excitation energy transfer from loosely bound LHCII to PSI in WT plants.

Introduction

In oxygenic photosynthesis photosystems I (PSI) and PSII work in series to oxidize water and reduce $NADP^+$. Both photosystems are composed of a core complex, which comprises the reaction center (RC) and the electron transport chain, and an outer light-harvesting (antenna) system (Blankenship, 2014; Croce and van Amerongen, 2020). In vascular plants the outer antenna of PSI, light-harvesting complex I (LHCI), is composed of four Lhca complexes, called Lhca1-4 (Knoetzel et al., 1992; Jansson et al., 1997;

Open Access

Jansson, 1999; Croce et al., 2002; Ben-Shem et al., 2003; Wientjes and Croce, 2011). The light-harvesting cross-section of the PSII core is enlarged by the monomeric CP24 (Lhcb6), CP26 (Lhcb5), and CP29 (Lhcb4) and trimeric LHCII complexes (combinations of Lhcb1-3; Jansson et al., 1997; Jansson, 1999). A special pool of LHCII trimers can associate with either PSI or PSII based on the light conditions (Allen et al., 1981; Bassi et al., 1988). PSI and PSII are both embedded in the thylakoid membrane, but their distribution is very heterogeneous. PSII is mainly found in the stacked grana membranes, while PSI is mainly located in the interconnecting unstacked stroma lamellae membranes (Andersson and Anderson, 1980; Dekker and Boekema, 2005).

As PSI and PSII work in series, a balanced excitation distribution between the two photosystems is required for optimal photosynthetic efficiency. However, PSI and PSII have different absorption spectra and during the day the light spectral composition can change depending on the time of the day and the position of the leaf in the canopy (Croce and van Amerongen, 2014; Johnson and Wientjes, 2020). At twilight, when the sun sets below the horizon, the ambient light becomes relatively enriched with colors of shorter wavelengths due to the increased amount of ozone absorption (Spitschan et al., 2016). Blue light of 460–490 nm is more readily absorbed by PSII, thus resulting in overexcitation of this photosystem when it is in state 1. Instead, below a canopy the blue and red part of the sun light is absorbed by upper leaves and the spectrum is enriched in green and far-red light. The red forms of PSI absorb the light above 700 nm, thus resulting in overexcitation of this photosystem (Coombe, 1957; Hogewoning et al., 2012; Johnson and Wientjes, 2020).

State transitions form the well-known acclimation mechanism that rebalances the excitation pressure on the photosystems by relocating LHCII between PSI and PSII (Allen, 2003; Rochaix, 2014; Goldschmidt-Clermont and Bassi, 2015). When PSII is overexcited the STN7 kinase phosphorylates the Lhcb2 isoform in the mobile pool of LHCII trimers (Lhcb1$_2$Lhcb2$_1$). The STN7 phosphorylated LHCII complex moves to PSI (State 2), where it binds to the PsaL/H/O site of the PSI core and forms a digitonin-resistant PSI–LHCI–LHCII complex (Bellafiore et al., 2005; Kouril et al., 2005; Galka et al., 2012; Crepin and Caffarri, 2015; Longoni et al., 2015; Pan et al., 2018). Instead, when PSI receives too much excitation energy, the LHCII is dephosphorylated by the TAP38/PPH1 phosphatase and moves to PSII (State 1; Pribil et al., 2010; Shapiguzov et al., 2010). State transitions are essential for plant fitness and maintaining a proper photosynthetic efficiency (Lunde et al., 2000; Bellafiore et al., 2005; Frenkel et al., 2007; Tikkanen et al., 2010; Taylor et al., 2019).

The nomenclature, State 1 and State 2, might give the impression that there are only two absolute states; however, this is not the case. While State 1 can be described as the condition where LHCII is not phosphorylated and digitonin stable PSI–LHCI–LHCII complexes are absent, this is not the same for State 2. Under most of the light regimes usually experienced by plants, part of the "extra" LHCII pool is phosphorylated and enlarges the PSI antenna in the PSI–LHCI–LHCII supercomplex, thus resulting in a "partial" State 2 (Tikkanen et al., 2008; Wientjes et al., 2013). Yet, illuminating the leaves with light that specifically overexcites PSII e.g. ∼470-nm or ∼650-nm light (Hogewoning et al., 2012), leads to a more "extreme" State 2.

Besides the association of one LHCII trimer with PSI in State 2, several reports indicate that unphosphorylated (digitonin sensitive) LHCII can function as PSI antenna in State 1 (Benson et al., 2015; Bressan et al., 2018; Bos et al., 2019) and that more than one LHCII complex can increase the PSI absorption cross section (Bassi and Simpson, 1987; Andreasson and Albertsson, 1993; Jansson et al., 1997; Bell et al., 2015; Benson et al., 2015; Grieco et al., 2015; Bos et al., 2017, 2019; Bressan et al., 2018; Chukhutsina et al., 2020). As mutant plants devoid of specific Lhcas also show impaired state-transitions, it has been suggested that these "additional" non-PsaH/L/O binding LHCII trimers transfer energy to the LHCI-site of PSI–LHCI (Benson et al., 2015). However, a subsequent study on ΔLhca Arabidopsis (*Arabidopsis thaliana*) plants, that lack all four Lhca antennas, showed that the thylakoid architecture of these plants is substantially modified with respect to the WT. It was concluded that the altered thylakoid organization makes the chlorophyll fluorescence analysis of state transitions problematic (Bressan et al., 2018). As such, it is at present not clear if the "additional" LHCII trimers indeed transfer their excitation energy to the LHCI site of PSI–LHCI, let alone how fast and efficient this energy transfer is.

In this work, we investigate the role of LHCI in mediating the energy transfer from LHCII to PSI in the stroma lamellae membranes. To this end, we compared the PSI antenna size and excitation energy transfer and trapping in State 1 versus State 2 membranes from wild-type (WT) and ΔLhca A. thaliana plants.

Results

State transitions and changes of the PSI antenna size

In order to investigate the role of LHCI in state transitions, we analyzed thylakoids purified from detached leaves of WT, ΔLhca, and Stn7ΔLhca plants after illumination of 45 min with far-red light (State 1) or orange light (State 2), in order to overexcite, respectively, PSI and PSII. Thylakoids from these plants were isolated and the chlorophyll *a/b* ratio was measured (Table 1). The chlorophyll *a/b* ratio of the WT and mutant plants were not affected by the 45-min light treatment, indicating that the PSI/PSII ratio and LHCII/PSII ratio did not change during the treatment. The thylakoids were solubilized with digitonin and the supernatant was analyzed using native polyacrylamide gel electrophoresis (PAGE; Figure 1). Digitonin is a mild detergent, which solubilizes the unstacked parts of the thylakoid membrane and preserves the binding interaction between the P-Lhcb2$_1$–

Table 1 PSI functional antenna size and chlorophyll *a/b* ratios of WT, Δ*Lhca*, and *Stn7ΔLhca* plants

Sample	WT	Δ*Lhca*	*Stn7ΔLhca*
		Chlorophyll *a/b* ratio	
State 1	2.81 ± 0.11	3.07 ± 0.04	2.75 ± 0.09
State 2	2.84 ± 0.09	3.03 ± 0.08	2.78 ± 0.11
		PSI functional antenna size	
State 1, %	100 ± 5.6[a]	79 ± 5.4[c]	81 ± 6.6[c]
State 2, %	130 ± 7.5[b]	104 ± 5.8[a]	81 ± 4.7[c]

For the chlorophyll *a/b* ratio the standard deviation of three measurements is indicated. The PSI antenna size is based on the P700 oxidation kinetics and expressed as percentage of the antenna size of WT State 1. The superscripts a–c indicate significantly different values (ANOVA, *P* < 0.02), based on five repetitions per sample and two biological replicates.

Lhcb1$_2$ trimer and the PsaH/L/O side of the PSI core (Zhang and Scheller, 2004; Kouril et al., 2005; Galka et al., 2012; Pan et al., 2018). After illumination with far-red light the PSI–LHCI–LHCII complex is absent in WT plants, and the PSI$_{core}$–LHCII complex is absent in Δ*Lhca* plants. Instead, illumination with orange light resulted in the association of LHCII to about 50% of the PSI–LHCI complexes in WT plants. Almost all PSI was found in the PSI$_{core}$–LHCII complex of Δ*Lhca* plants, in agreement with previous results (Bressan et al., 2016). As expected, the PSI$_{core}$–LHCII complex was not observed in *Stn7ΔLhca* plants, which lack the LHCII kinase required for the phosphorylation of Lhcb2–Lhcb1$_2$. It can be concluded that State 1 and State 2 were successfully induced in the WT and Δ*Lhca* plants, while *Stn7ΔLhca* plants were locked in State 1.

To evaluate the functional PSI antenna size in intact thylakoids, the P700 oxidation kinetics was followed by absorption spectroscopy (Figure 2 and Table 1). In State 1 the PSI antenna size was 79% ± 5% for Δ*Lhca* plants and 81% ± 7% for *Stn7ΔLhca* plants, relative to 100% for WT State 1 plants. The smaller PSI antenna size of Δ*Lhca* plants is consistent with the lack of LHCI in this mutant. Moving to State 2 increased the PSI antenna size by 30% ± 9% in the WT (Table 1) and by 25% ± 8% in Δ*Lhca*. The increase in antenna size of the Δ*Lhca* plants is comparable to that of WT plants, showing that LHCII is still capable of enlarging the functional antenna size of PSI in the absence of LHCI. No change in the antenna size is observed for *Stn7ΔLhca* plants, as is expected in the absence of STN7.

Sodium dodecyl sulphate–PAGE analysis of stroma lamellae membranes

In the stroma lamellae almost all the light is harvested by PSI and its antenna, while PSII is only present at very low levels (Andersson and Anderson, 1980; Bressan et al., 2018). This membrane fraction is therefore not only suitable to investigate how many LHCII trimers per PSI are present, but also to study how the energy transfers from these LHCII complexes to PSI in the presence (WT) and absence (Δ*Lhca*) of the LHCI system. For WT and Δ*Lhca* membranes the content of Lhcb1 and Lhcb2, which are the major components of the LHCII trimer, is clearly increased in State 2 relative to State 1 membranes (Figure 3). In line with the

greater abundance of chlorophyll *b*-rich LHCII complexes in State 2 membranes, the chlorophyll a/b ratio was decreased compared to State 1 (Figure 3). The densitometric analysis of the sodium dodecyl sulphate–PAGE (SDS–PAGE) was used to quantify the number of LHCII trimers per PSI (Table 2). In State 1, the PSI antenna systems were already endowed with 0.6 ± 0.1 LHCII trimers in WT, 0.6 ± 0.1 LHCII trimers in Δ*Lhca* and 0.5 ± 0.1 in *Stn7ΔLhca*. Upon going to State 2, this ratio increased to 1.6 ± 0.1 LHCII trimers/PSI in the WT and 1.8 ± 0.1 LHCII trimers/PSI in Δ*Lhca* stroma lamellae. Based on the analysis of the native gel, we estimate that roughly 0.5 LHCII trimers per PSI is associated at the PsaH/L/O site of the core in the digitonin stable PSI–LHCI–LHCII complex of WT State 2 thylakoids and almost 1 LHCII in the digitonin stable PSI$_{core}$–LHCII complex of Δ*Lhca* thylakoids. Assuming that this ratio is similar in stroma lamellae it follows that roughly 1 digitonin-sensitive LHCII per PSI is present in the WT and 0.8 LHCII per PSI in Δ*Lhca* State 2 stroma lamellae. As expected virtually no change of LHCII trimers per PSI was observed for the *Stn7ΔLhca* stroma lamellae between State 1 and State 2.

Excitation energy transfer and trapping in stroma lamellae membranes

Time-resolved fluorescence measurements using a streak-camera setup allowed us to follow the fluorescence intensity with picosecond time resolution as a function of emission wavelength. A fast decay of the fluorescence from PSI generally means that the excitation energy is quickly transferred to the RC, where it is trapped (Russo et al., 2020). The faster the energy is trapped by the RC the lower the possibility that the energy is lost by other competing processes and as such the higher the quantum yield of the photosystem. The fluorescence of PSI core complexes from plants decays in 20–25 ps (Slavov et al., 2008; Wientjes et al., 2011), which is two orders of magnitude faster than the ns decay of the isolated Lhc antenna, indicating that the quantum yield of charge separation is close to unity. The fluorescence lifetime of PSI–LHCI is longer due to three reasons. First, the number of chlorophyll *a* molecules per RC has increased, which leads to a longer average migration time from the antenna chlorophylls to the RC (van Grondelle and Gobets, 2004; Broess et al., 2006). Second, the probability that the excitation is located on the RC is lower for a larger antenna system, thus increasing the trapping time (Broess et al., 2006). Third, Lhca3 and Lhca4, which are part of LHCI, contain the so-called red-forms, chlorophylls that absorb light at longer wavelengths (lower energy) than the RC. The slower up-hill energy transfer from the red-forms to the RC further increases the fluorescence lifetime (Jennings et al., 2003). Nevertheless, the average lifetime of plant PSI-LHCI is only 50–60 ps (Croce et al., 2000; Ihalainen et al., 2005; Slavov et al., 2008; van Oort et al., 2008; Wientjes et al., 2011; Croce and van Amerongen, 2020), showing that its efficiency is still over 98%.
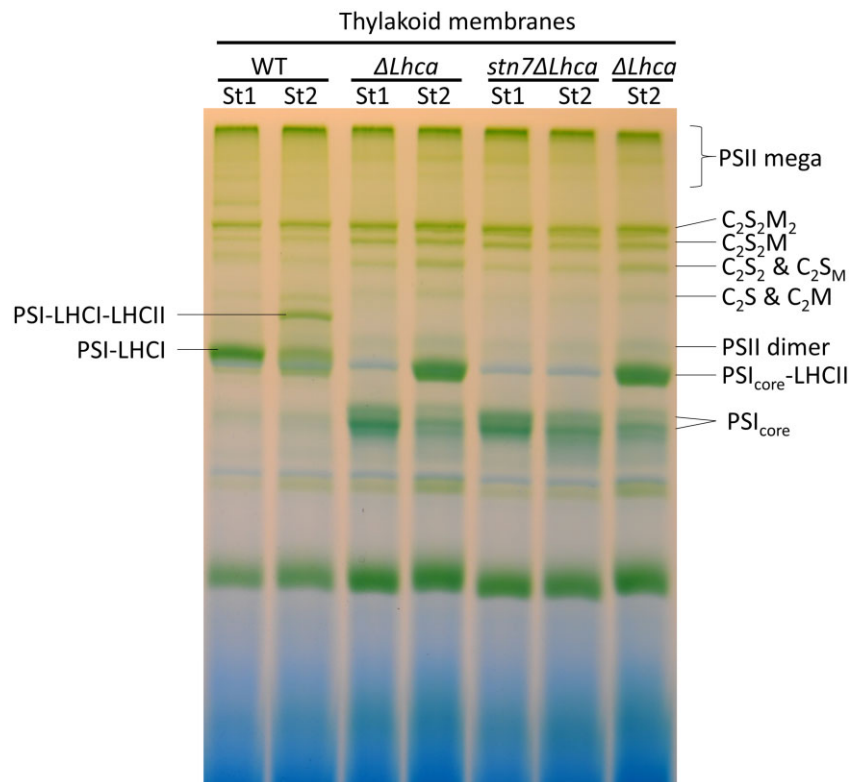
Figure 1 Organization of thylakoid pigment–protein complexes. Photosynthetic complexes from WT, Δ*Lhca*, and *Stn7*Δ*Lhca* were separated by nondenaturing Blue native polyacrylamide gel electrophoresis (BN–PAGE) following solubilization of membranes with 0.1% α-DM + 0.5% digitonin. The composition of major green bands is indicated based on earlier work (Jarvi et al., 2011). St, State, $C_2S_2M_2$, dimeric PSII core, with two strongly (S) bound LHCII and two moderately (M) bound LHCII complexes, C_2S_2M, C_2S_2, C_2S_2M, C_2S, and C_2M accordingly.

In order to investigate the role of LHCI in mediating energy transfer from LHCII to PSI, we performed streak-camera fluorescence decay measurements on the WT and Δ*Lhca* stroma lamellae membranes. In Figure 4A, the fluorescence intensity is depicted by the color scale, the vertical axis shows the time and the horizontal axis the wavelengths. Along the horizontal axis, one can see how the fluorescence spectrum changes at different time points after the excitation; as an example the white dashed line shows the average fluorescence spectrum from 70 to 90 ps after the laser pulse (indicated by the white dashed box). This spectrum of WT State 1 stroma lamellae membranes shows a strong shoulder around 715 nm, typical for PSI–LHCI. In WT State 2 membranes, the intensity of the peak at 680 nm is increased, in agreement with the increased LHCII content. In the Δ*Lhca* membranes the shoulder around 715 nm is absent due to the lack of the red forms of Lhca3 and Lhca4 (Croce et al., 2002). Along the vertical axis, the fluorescence intensity is followed over time. As an example, Figure 4, B and C shows the fluorescence decay traces of the WT and Δ*Lhca* membranes at 682 nm and 715 nm. In WT stroma lamellae membranes, the fluorescence decay around 715 nm is slower than around 682 nm, which can be readily explained by the slow up-hill energy transfer from the red forms (around 715 nm) to the bulk chlorophylls (around 682 nm; Jennings et al., 2003; Wientjes et al., 2011; Wientjes et al., 2011).

Instead the decay kinetics are almost independent of the wavelengths for the Δ*Lhca* membranes. Increasing the PSI antenna size with LHCII in State 2 slows down the fluorescence decay kinetics in both WT and Δ*Lhca* membranes, showing that it takes on average more time to transfer the excitation energy to the RC.

To make a quantitative comparison of the excitation energy transfer and trapping kinetics the data are described with decay-associated spectra (DAS). For each wavelength the fluorescence decay is described with a sum of exponentials: $F(t) = a_1 e^{-t/\tau 1} + a_2 e^{-t/\tau 2} + \cdots$, in which the lifetimes (τ) are the same for each wavelength and the amplitudes (a_n) are plotted as the DAS, showing how much each lifetime contributes to the fluorescence decay at that wavelength. In Figure 5, the DAS of the WT and Δ*Lhca* stroma lamellae after 400-nm excitation are compared to the decay of isolated PSI–LHCI (from Bos et al., 2017) and PSI core complexes (see "Materials and methods"). All samples have a spectrum associated with a short ∼5 ps lifetime, with both a maximum around 680–690 nm and a minimum around ∼715 nm. This represents excitation energy equilibration between bulk chlorophylls *a* and the low-energy-emitting chlorophylls *a* (red-forms) of the PSI core and especially of Lhca3 and Lhca4 (Wientjes and Croce, 2011). In PSI–LHCI the fluorescence decays with two lifetimes, a 26-ps component with a maximum at 680–690 nm and an 86-ps
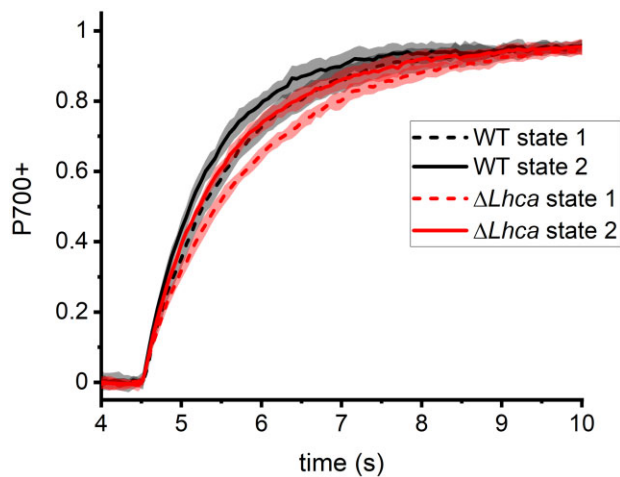
Figure 2 Functional PSI antenna size in intact thylakoids. P700 oxidation kinetics of WT and $\Delta Lhca$ thylakoids in State 1 and State 2 was followed by absorption spectroscopy ($\lambda = 830$–875 nm). The oxidation kinetics of $Stn7\Delta Lhca$ thylakoids, in both far-red and orange adapted leaves, overlapped with the $\Delta Lhca$ State 1 thylakoids.

Figure 3 Fractionation of thylakoid proteins by SDS–PAGE and chlorophyll a/b ratio of WT, $\Delta Lhca$, and $Stn7\Delta Lhca$ stroma lamellae membranes. The region of the $Lhcs$ and the PsaD PSI core polypeptides are shown, as indicated in the figure. Contrast is enhanced for improved clarity. St1, State 1; St2, State 2, Chl a/b, chlorophyll a/b ratio.

Table 2 Number of LHCII trimers per PSI in WT, $\Delta Lhca$, and $Stn7\Delta Lhca$ stroma lamellae membranes based on the SDS–PAGE gel

LHCII trimer/PSI	WT	$\Delta Lhca$	$Stn7\Delta Lhca$
State 1	0.58 ± 0.08	0.55 ± 0.06	0.53 ± 0.13
State 2	1.64 ± 0.09	1.80 ± 0.11	0.62 ± 0.12
State 2–State 1	1.06 ± 0.12	1.25 ± 0.13	0.1 ± 0.2

The standard deviation of four replicas from two biological samples is provided.

component with a red-shifted emission maximum of $\sim$ 715 nm. The WT State 1 stroma lamellae with 0.6 LHCII trimers per PSI show increased emission around 680 nm in the 37-ps and 121-ps DAS when compared with the 26-ps and 86-ps DAS of isolated PSI–LHCI complexes. Indeed, an increase in amplitude at 680 nm is expected as this is the emission maximum of LHCII. Furthermore, all stroma lamellae DAS show a $\sim$1 ns component with a maximum at 680 nm, which is ascribed to PSII core complexes that are known to be present in stroma lamellae membranes (Andersson and Anderson, 1980). Upon transitioning to State 2 the number of LHCII complexes per PSI increase to 1.6, this results in a further relative increase in the DAS around 680 nm. The average PSI–LHCII$_n$ fluorescence lifetime increases from 89 ± 8 ps in WT State 1 stroma lamellae membranes to 102 ± 4 ps in State 2 (Table 3). The average increase in lifetime (State 2–State 1) is 14 ± 4 ps (Table 3), which can be ascribed to the increase in antenna size with 1.1 LHCII trimers (Table 2). This increase of the lifetime is due to the increased trapping time plus the LHCII to PSI migration time (Broess et al., 2006). Based on the absorption spectra and the number of chlorophylls per complex the additional LHCIIs absorb 19% of the light at 400 nm (Supplemental Figure S1). If all excitations would occur in LHCII the increase in lifetime would have beenhttp://doi.org/ (van Oort et al., 2008), setting the limit for the average time it takes to transfer excitation energy from the extra State 2 LHCIIs to PSI to a maximum of 74 ± 21 ps.

The fluorescence decay of the PSI core could be described with one lifetime of 29 ps. A small 4 ns contribution was also present, but this can be attributed to a contamination of uncoupled light-harvesting complexes and/or free chlorophylls. In the $\Delta Lhca$ State 1 stroma lamellae membranes the PSI core antenna size is enlarged by 0.6 LHCII trimers. These LHCII trimers contribute mainly to the new DAS with a
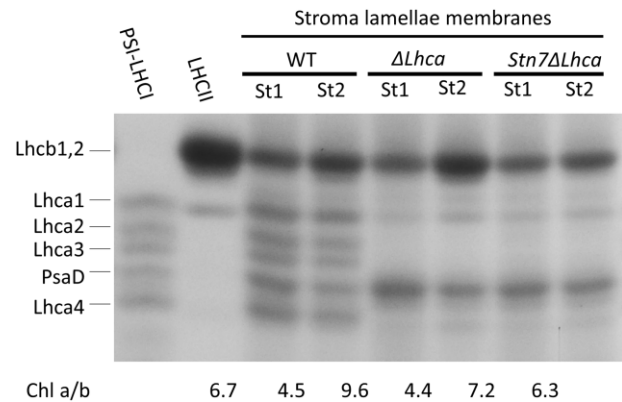
lifetime of 221 ps. In State 2, the shortest trapping lifetime increases from 29 ps to 50 ps, clearly indicating that LHCII influences this component. In addition, a 200-ps DAS strongly contributes to the decay (Figure 5). In State 2, $\Delta Lhca$ membranes the LHCII/PSI ratio is increased by 1.3 LHCII trimers compared to State 1. The additional State 2 LHCII is responsible for 28% of the 400 nm light absorption. The average lifetime of State 2 compared to State 1 membranes is 34 ± 4 ps longer (Table 3). It can thus be estimated that the sum of the increased trapping time and the transfer time from the additional LHCIIs to the PSI core is . The DAS of State 1 and State 2 $Stn7\Delta Lhca$ membranes look very similar to that of $\Delta Lhca$ State 1 membranes, with a small increase in the amplitude of the $\sim$200 ps component in State 2 (Supplemental Figure S2).

Discussion

How fast and efficient does LHCII transfer energy to PSI?

In recent years evidence accumulated which suggests that LHCII operates as PSI antenna, not only in State 2, but also in State 1 (Benson et al., 2015; Grieco et al., 2015; Bressan et al., 2018; Bos et al., 2019; Chukhutsina et al., 2020). In this work, we investigated how efficient LHCII transfers energy to PSI in stroma lamellae membranes, with the emphasis on the role of LHCI in mediating energy transfer from LHCII to PSI. In $\Delta Lhca$ membranes, devoid of LHCI, a decay component with a lifetime of 221 ps was attributed to LHCII in the
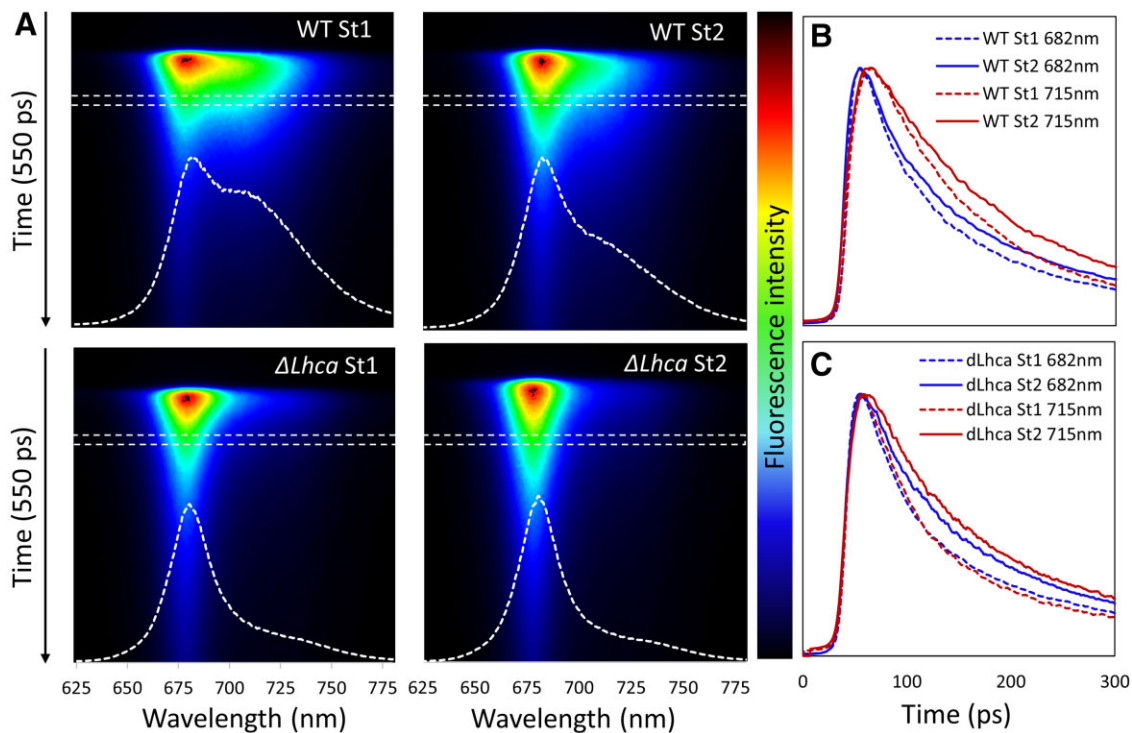
Figure 4 Streak-camera fluorescence decay measurements of WT and $\Delta Lhca$ State 1 and State 2 stroma lamellae membranes. Excitation was at 400 nm. A, Streak-camera images and the fluorescence spectra 70–90 ps after the laser pulse. The white dashed lines show the fluorescence emission spectra at the time-interval indicated with the white dashed boxes. B, C, Fluorescence decay kinetics of WT (B) and $\Delta Lhca$ (C) State 1 and State 2 membranes at 682 ± 3 nm and 715 ± 3 nm. The fluorescence decay of State 2 membranes is slower than that of State 1 membranes for both WT and $\Delta Lhca$ stroma lamellae.

Table 3 Average fluorescence lifetime of PSI–LHCII complexes in the stroma lamellae

Average lifetime	WT	$\Delta Lhca$	Stn7 $\Delta Lhca$
State 1	89 ± 8 ps	67 ± 10 ps	75 ± 9 ps
State 2	102 ± 4 ps	93 ± 14 ps	90 ± 10 ps
State 1–State 2	14 ± 4 ps	34 ± 4 ps	15 ± 3 ps

The average fluorescence lifetimes were calculated based on the relative area of the DASs colored red and blue in figure 5, whereas the ~1 ns lifetime attributed to PSII core fluorescence was not taken into account. The standard deviation is provided based on three measurements; the stroma lamellae membranes were isolated twice form different batches of plants. One set of samples was measured twice on different days and the other set was measured once. The difference in lifetimes between State 1 and State 2 was calculated based on one set of measurements and then averaged for the three replicates. Excitation was at 400 nm.

results section. The total decay rate of $1,000/221 = 4.5$ ns^{-1} is the sum of the LHCII to PSI transfer rate and the intrinsic LHCII decay rate ($k_{tot} = k_{transfer} + k_{intrin\ decay}$). The intrinsic decay rate of LHCII in a membrane is hard to determine as it strongly depends on its aggregation state. Lifetimes between 1 ns and 3 ns were measured for LHCII in liposomes (corresponding to rates of 1–0.33 ns^{-1}), depending on the protein to lipid ratio (Natali et al., 2016), and an average rate of 1.7 ns^{-1} has been determined for disconnected LHCIIs in the CP24 knockout mutant (van Oort et al., 2010) and for lamellar LHCII aggregates (Miloslavina et al., 2008). As we assume that the LHCII complexes in the stroma lamellae are not aggregated we will use a value of 0.5 ns^{-1}, as

it has been used before in LHCII to PSI energy transfer studies (Akhtar et al., 2016; Santabarbara et al., 2017). This gives a rate of: $k_{transfer} = k_{tot} - k_{intrin\ decay} = 4.5 - 0.5 = 4$ns^{-1} (or a transfer time of 250 ps), for the unphosphorylated LHCII to PSI core energy transfer in State 1 $\Delta Lhca$ stroma lamellae. In State 2, $\Delta Lhca$ membranes, the PSI antenna size is increased by 1.3 LHCII trimers to 1.8 LHCII/PSI core, of which one is present in the digitonin stable PSI$_{core}$–LHCII complex. The other 0.8 LHCII likely interact with the PSI core on other, yet unidentified, location(s). The newly arising 50-ps decay component (Figure 5) is reminiscent of the main 58-ps decay component observed for digitonin isolated PSI$_{core}$–LHCII complexes after excitation with 475-nm light, which is strongly absorbed by LHCII (Bressan et al., 2016). It is therefore likely to be due to the energy transfer from the phosphorylated Lhcb1$_2$Lhcb2$_1$ trimer to the PsaH/L/O site of the PSI core and occurs with a rate of: $k_{transfer} = k_{tot} - k_{intrin\ decay} = \frac{1000}{58} - 0.5 = 16.7$ ns^{-1} (transfer time of 60 ps). This is consistent with previous energy transfer studies on isolated PSI–LHCI–LHCII complexes which showed an increased amplitude in the 30–40 ps and 80–100 ps components, relative to PSI–LHCI (Galka et al., 2012; Wientjes et al., 2013). Similar transfer times in the order of 60 ps where observed for LHCII to PSI transfer in spinach (*Spinacia oleracea*) PSI–LHCII membranes (Bos et al., 2017) and in PSI–LHCI–Lhcb$_7$ supercomplexes from *Chlamydomonas reinhardtii* (Le Quiniou et al., 2015). It is also in agreement
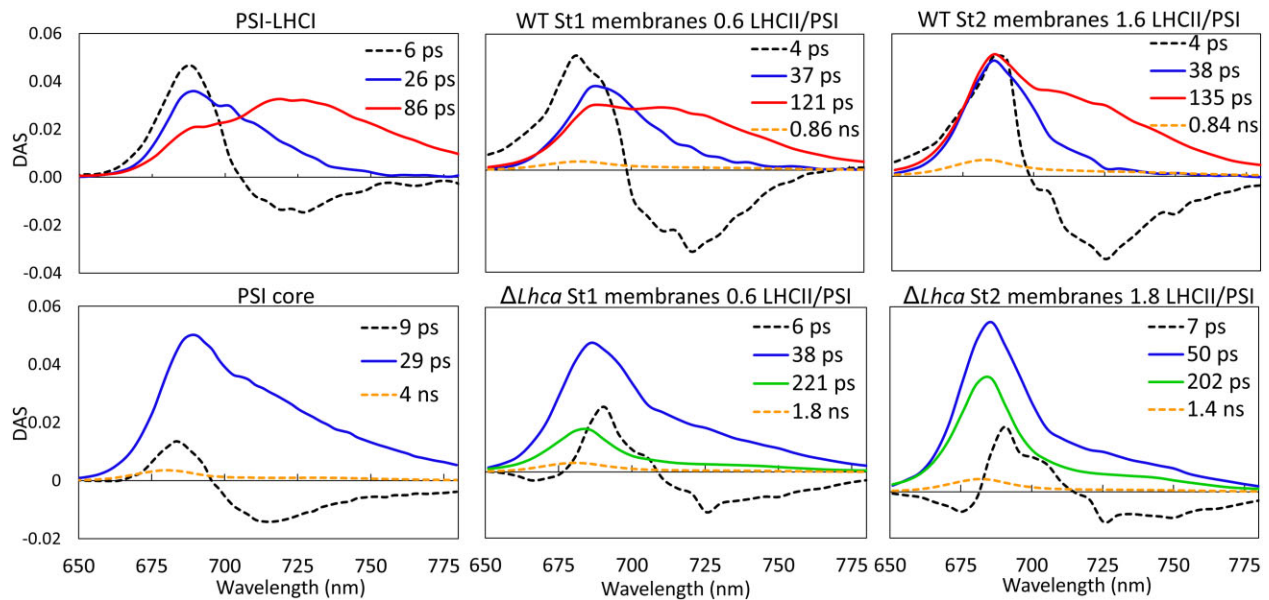
Figure 5 DAS of PSI–LHCI, PSI core, State 1 (St1) and State 2 (St2) WT, and ΔLhca stroma lamellae membranes. Excitation was at 400 nm. The number of LHCII complexes per PSI, based on the SDS–PAGE analysis, is indicated in the figure.

with the 15 ns^{-1} transfer rate observed for 20% of the LHCII to PSI transfer based on kinetic modeling of isolated PSI–LHCI–LHCII decay (Santabarbara et al., 2017). However, it is considerably slower than the main LHCII to PSI transfer component of 55 ns^{-1} found in the same study (Santabarbara et al., 2017). We note that based on our work, the presence of a pool of fast transferring PsaH/L/O-LHCII cannot be entirely excluded, as it would mix with the PSI core trapping kinetics. The other, "additional" LHCII trimer present in the State 2 ΔLhca membranes contributes to the ∼200 ps decay component, indicating rather slow LHCII to PSI energy transfer.

To get a better idea of the LHCII to PSI energy transfer rates we modeled the time-resolved fluorescence data with minimal schemes (Supplemental Text S1). For the State 1 ΔLhca stroma lamellae membranes we used one LHCII pool and one PSI core pool, which were able to transfer energy to each other (obeying the detailed balance equation for backward and forward rates) and also decayed with their own rates (0.5 ns^{-1} for LHCII and 33 ns^{-1} for the PSI core). The wavelength-dependent fluorescence decay kinetics was based on the decay kinetics of the individual pools and the known emission spectra (Supplemental Figure S3). From these data the DAS were calculated and compared to the original data. The LHCII to PSI core transfer rate of 4 ns^{-1} (vida supra) did indeed yield a DAS similar to our measurements. For the State 2 ΔLhca membranes, we used 16.7 ns^{-1} for the digitonin stable PsaH/L/O-LHCII and obtained the best results with a transfer rate of 3.8 ns^{-1} for the additional digitonin-sensitive LHCII (Supplemental Figure S4).

For WT stroma lamellae it is not possible to extract the LHCII to PSI–LHCI transfer times directly from the DAS as they are very similar to the PSI–LHCI trapping times and are therefore not resolved separately. However, based on the

increase in the average lifetime upon State 1 to State 2 transition, it was calculated that the sum of the increased trapping time and the LHCII to PSI migration time was 76 ± 22 ps, meaning that the 1.1 extra LHCII complexes transfer their energy to PSI in less than this time. To model these data red forms, responsible for the long-wavelength emission of Lhca3 and Lhca4 (Schmid et al., 1997; Croce et al., 2002; Castelletti et al., 2003; Wientjes and Croce, 2011), were added as a pigment pool (Supplemental Figure S5). An LHCII to PSI core transfer rate of 8 ns^{-1} (transfer time of 125 ps) gave the best results for the State 1 WT membranes (Supplemental Figure S6). For State 2 WT membranes, the best results were obtained when the digitonin-sensitive LHCII transferred its energy with a rate of 8 ns^{-1} to the red forms of LHCI. However, a transfer rate of 7.6 ns^{-1} to the bulk pigment pool of LHCI and the PSI core gave comparable results (Supplemental Figure S7). Based on these data, we cannot conclude if the digitonin-sensitive LHCII transfers its energy mainly to Lhca3/Lhca4, or rather to Lhca1/Lhca2. However, as the LHCII to PSI core transfer in the ΔLhca membranes was twice as slow, it shows that LHCI has a role in mediating energy transfer from LHCII to PSI, probably by having LHCII binding positions, which allow for short Chlorophyll–Chlorophyll distances, favorable for Förster resonance energy transfer. Instead the energy transfer from "additional" LHCII complexes to PSI in the ΔLhca mutant is probably caused by random interaction with the core, similar to what happens when PSI and PSII mix and excitation energy spills over from PSII to PSI (Anderson, 1999).

Figure 6 gives a schematic overview of the transfer rates and number of LHCII trimers per PSI in WT and ΔLhca stroma lamellae. The width of the arrow indicates the speed of excitation energy transfer. The efficiency of excitation energy transfer can be approximated from the transfer rate
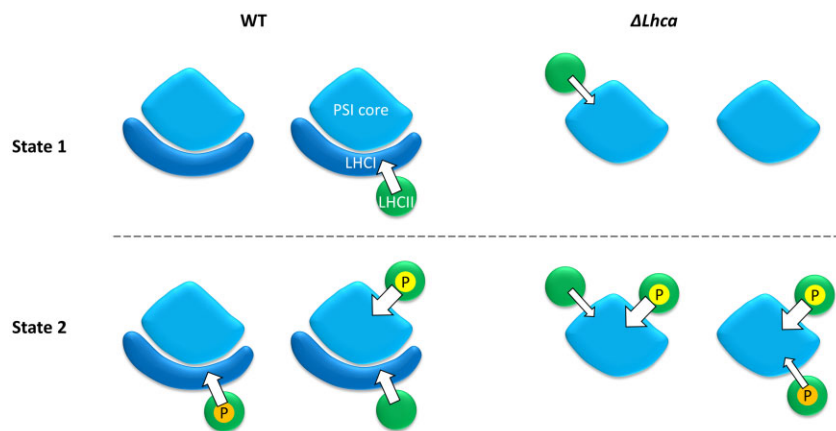
Figure 6 Rate of energy transfer from LHCII to PSI in State 1 and State 2 stroma lamellae membranes from WT and Δ*Lhca* plants. The width of the arrow represents the rate of the energy transfer. The number of LHCII trimers per PSI complex is based on the SDS–PAGE data. Color coding: green–LHCII trimer; light blue–PSI core; dark blue– LHCI; P in yellow circle–phosphate group on Lhcb2 associating with the PsaH site of the PSI core; P in orange circle–phosphate group on digitonin-sensitive LHCII.

divided by the total decay rate of the LHCII involved. For the digitonin-sensitive LHCII complexes in the Δ*Lhca* mutant this is 89% (transfer rate of 4 ns^{-1}), while it is 94% efficient in the WT (transfer rate 8 ns^{-1}). The PsaH/L/O LHCII has the highest transfer efficiency of 97%. The expected phosphorylation states are also indicated in Figure 6. As LHCII is not phosphorylated in State 1 membranes, we hypothesize that this pool of LHCII remains unphosphorylated in State 2 membranes. Instead, the "additional" LHCII that moves to the stroma lamellae membranes upon State 2 induction are phosphorylated.

How much are state transitions affected in the Δ*Lhca* mutant?

When evaluating state transitions with a pulse–amplitude–modulation (PAM) chlorophyll fluorometer, the change in the PSII antenna size by state transitions is reduced to 31% (Benson et al., 2015) or even 13% (Bressan et al., 2018) in the Δ*Lhca* mutant relative to WT levels. Instead, judged by the P700 oxidation kinetics, the change in the PSI antenna size in the Δ*Lhca* mutant is only reduced to 61% (Benson et al., 2015) or 83% (this work). Furthermore (Wood et al., 2019) showed that a change in grana size as a result of LHCII phosphorylation still occurs in Δ*Lhca4* plants, indicating that LHCII relocation does happen in the absence of LHCI. Even more, the increase in number of LHCII complexes per PSI upon transitioning from State 1 to State 2 is similar for the stroma lamellae membranes from Δ*Lhca* and WT plants. These seemingly contradictory observations probably arise from a combination of at least two factors. First, the far-red 720 nm LED source used in the PAM to overexcite PSI is probably not strong enough to fully induce State 1 in Δ*Lhca* plants, as they lack most of the red-forms, which are located in LHCI. This light source will be especially ineffective when used in combination with orange or red light, which overexcites PSII as used by (Benson et al., 2015; Bressan et al., 2018). Instead, the change in the PSI antenna

size was estimated from measurements on thylakoids that were isolated from leaves illuminated by far-red light only for at least 45 min, to induce State 1, or red/orange light to induce State 2 (Benson et al., 2015 and this work). Second, the relocation of LHCII during state transitions could be affected in the Δ*Lhca* mutant by a change of the thylakoid ultrastructure (Bressan et al., 2018). A previous membrane fractionation study showed that in WT plants the transition from State 1 to State 2 resulted in an increase of LHCII in the margins and stroma lamellae fraction at the cost of LHCII in the grana fraction. Instead, in Δ*Lhca* plants LHCII only moved from the grana to the stroma lamellae fraction (Bressan et al., 2018). Taken together, it can be concluded that the presence of LHCI is not a requirement for the successful relocation of LHCII between grana and stroma lamellae membranes, nor for excitation energy transfer from mobile LHCII to the PSI core.

Regulation of LHCII movement

This work further supports the recent observations that in State 1 unphosphorylated LHCII enlarges the antenna of PSI in *A. thaliana* (Benson et al., 2015; Bressan et al., 2018; Bos et al., 2019). Future research needs to point out how the distribution of this unphosphorylated LHCII between the grana and stroma lamellae membranes is regulated. One possible mechanism is the reversible acetylation of LHCII lysines. Acetylation of a lysine neutralizes the positive charge, as such increasing the net negative charge of the LHCII surface. The increased negative charge of phosphorylated LHCII is one of the suggested mechanisms, which drives the dissociation of LHCII from PSII, after which it can move to PSI (Allen, 1992). It has already been shown that lysine acetylation plays a role in state transitions, as *A. thaliana* plants which lack the lysine acetyltransferase, NSI, cannot form the PSI–LHCI–LHCII supercomplex under State 2 conditions (Koskela et al., 2018).

In conclusion, LHCI is not required for the "additional" non-PsaH/L/O binding LHCII trimers to transfer energy to PSI; however LHCI does facilitate fast and therefore efficient excitation energy transfer to PSI.

Materials and methods

Plant material and growth conditions

WT plants of Arabidopsis (*A. thaliana*; Col-0), mutant Δ*Lhca* (Bressan et al., 2018), and double mutant *stn7ΔLhca*, obtained by crossing the *stn7* mutant (Bellafiore et al., 2005) with the Δ*Lhca* mutant (Bressan et al., 2018), were grown for 6 weeks at 150 μmol photons m^{-2} s^{-1}, 8 h of daylight (OSRAM halogen HQI-T 250W and/or OSRAM lumilux cool white L58W) and 23°C/20°C day/night at a humidity of 70%.

Thylakoid and stroma lamellae isolation

State 1 and State 2 were induced as in Bressan et al. (2018) with slight modifications; leaves from overnight dark-adapted plants were placed on wet paper for 45 min with either PSI light (a combination of far-red LEDs with a peak at 730 nm and 850 nm) or PSII light (30-W warm white fluorescent lamps filtered with Lee 105 orange filters). Thylakoids were isolated as previously described (Berthold et al., 1981). Leaves treated with State 1 or State 2 light were directly homogenized using ice-cold buffer B1 (20-mM tricine-KOH, pH 7.8, 0.4-M NaCl, 2-mM MgCl$_2$, 0.5% milk powder) and filtered with a nylon mesh before centrifugation at 1,500g, 4°C for 12 min. The pellet was washed in buffer B2 (20-mM tricine-KOH, pH 7.8, 0.15-M NaCl, 5-mM MgCl$_2$) before centrifugation at 4,000g, 4°C for 12 min. The pellet was resuspended in buffer B3 (20-mM HEPES-KOH, pH 7.5, 15-mM NaCl, 5-mM MgCl$_2$) and centrifuged at 6,000g, 4°C for 12 min. If thylakoids were stored, they were resuspended in buffer B4 (20-mM HEPES-KOH, pH 7.5, 0.4-M sorbitol, 15-mM NaCl, 5-mM MgCl$_2$) and immediately frozen in liquid nitrogen before storage at −80°C. Buffer B1–B3 were supplemented, right before grinding or resuspending, with protease inhibitors (0.1-mM benzamidine, 0.1-mM PMSF, 0.5-mM aminocaproic acid) and freshly prepared 10-mM sodium fluoride. Stroma lamellae isolation was performed as previously described (Barbato et al., 2000), from freshly prepared thylakoids in buffer B3. Solubilized thylakoids were seven times diluted with buffer B3 before the centrifugation steps.

PSI core isolation

Arabidopsis thaliana ch1 plants (ordered from TAIR database: CS126), which lack chlorophyll *b* and accumulate the PSI core without LHCI associated (Havaux et al., 2007), were grown as described above and the thylakoids were isolated. Thylakoids at a chlorophyll concentration of 1 mg·mL^{-1} were dissolved with an equal volume of 1.2% (w/v) n-dodecyl β-ᴅ-maltoside. After 5-min incubation on ice the mixture was centrifuged for 1 min at 13,000g and the supernatant was loaded on a 0.1–1 M sucrose density gradient as

described in Wientjes et al. (2009). The bands were harvested with a syringe and the PSI core band (monomeric and oligomeric state) were identified based on position in the gradient, chlorophyll content, and absorption spectra.

Normalization of absorption spectra

The absorption spectra of LHCII, PSI–LHCI (Hogewoning et al., 2012), and PSI core were normalized to respectively 42, 155, and 98 chlorophylls (Liu et al., 2004; Qin et al., 2015) taking into account the chlorophyll *a/b* ratios of 1.3 (LHCII), 11.9 (PSI–LHCI), and ∞ (PSI-core) and an oscillator strength for chlorophyll *b* of 0.7 times chlorophyll *a* in the region from 630 to 750 nm (Sauer et al., 1966).

Pigment analysis

The pigment composition of the different states were analyzed by fitting the acetone extract spectrum with the spectra of the individual pigments as described (Croce et al., 2002).

PSI antenna size measurements

P700 measurements were performed as described before (Benson et al., 2015) on a Walz DUAL-PAM-100 in the dual wavelength mode (830 and 875nm) using a concentration of 50-μg chlorophylls per mL in the measuring buffer (0.4-M sorbitol, 15-mM NaCl, 5-mM MgCl$_2$, 10-mM HEPES, pH 7.5, buffered KOH, 50-μM DCMU, 100-μM methylviologen, 500-μM sodium ascorbate). The following protocol was used for five cycles on every sample: 5-s dark, 10-s red light (635 nm) at 6-μmol photons m^{-2} s^{-1}, and 30-s dark recovery. Traces were normalized between the minimum (beginning of each cycle) and the maximum and fitted with an exponential function to determine the $t_{1/2}$ for the antenna size calculations. PSI antenna sizes are expressed as a percentage of the WT State 1 value.

Polyacrylamide gel electrophorese

For the large pore-blue native gel the samples and gels were prepared as described (Jarvi et al., 2011), and solubilization of samples was carried out with 0.1% α-DM and 0.5% digitonin final concentration as described previously (Galka et al., 2012). In total, 40 μg of chlorophylls were loaded in a medium-sized gel (16 cm height). For the SDS–PAGE, a modified Laemmli gel was used as described in Laemmli (1970) and Ballottari et al. (2004).

Streak-camera measurements

Time-resolved fluorescence measurements were performed with a streak-camera system as described previously (van Stokkum et al., 2008; van Oort et al., 2009). The sample was measured in a 1 cm × 1 cm cuvette at a chlorophyll concentration of 20 μg·mL^{-1} and continuously stirred during the measurement. To excite the sample, pulsed laser light with a repetition rate of 3.8 MHz, a wavelength of 400 nm and an intensity of ~50 μW, was focused in a spot with a diameter of ~100 μm. Time windows of 2 ns and 800 ps were used for the measurements. The collected streak

images were corrected for background signal and for spatial variation of detection sensitivity. The corrected data sets were globally analyzed using Glotaran and described with decay-associated spectra (Mullen and van Stokkum, 2007; Snellenburg et al., 2012).

Accession numbers

Sequence data from this article can be found in the GenBank/EMBL data libraries under accession numbers AT3G5489- (*Lhca1*), AT3G61470 (*Lhca2*), AT1G61520 (*Lhca3*), AT3G47470 (*Lhca4*), AT1G68830 (*STN7*)._.

Supplemental data

The following materials are available in the online version of this article.

Supplemental Figure S1. Absorption spectra of PSI–LHCI, PSI core, and LHCII trimer.

Supplemental Figure S2. DAS of *Stn7ΔLhca* stroma lamellae membranes.

Supplemental Figure S3. Kinetic modeling approach.

Supplemental Figure S4. Kinetic modeling of *ΔLhca* stroma lamellae excited-state kinetics.

Supplemental Figure S5. Kinetic modeling of PSI–LHCI.

Supplemental Figure S6. Kinetic modeling of WT State 1 stroma lamellae excited state kinetics.

Supplemental Figure S7. Kinetic modeling of WT State 2 stroma lamellae excited state kinetics.

Supplemental Table S1. Initial excitation of the compartments used for the kinetic modeling.

Supplemental Table S2. Detailed balance equation for the compartments used for the kinetic modeling.

Supplemental Text S1. Kinetic modeling.

Acknowledgments

Funding

References

Akhtar P, Lingvay M, Kiss T, Deak R, Bota A, Ughy B, Garab G, Lambrev PH (2016) Excitation energy transfer between Light-harvesting complex II and Photosystem I in reconstituted membranes. Biochim Biophys Acta **1857:** 462–472

Allen JF (1992) How does protein-phosphorylation regulate photosynthesis. Trends Biochem Sci **17:** 12–17

Allen JF (2003) State transitions - a question of balance. Science **299:** 1530–1532

Allen JF, Bennett J, Steinback KE, Arntzen CJ (1981) Chloroplast protein-phosphorylation couples plastoquinone redox state to distribution of excitation-energy between photosystems. Nature **291:** 25–29

Anderson JM (1999) Insights into the consequences of grana stacking of thylakoid membranes in vascular plants: a personal perspective. Aust J Plant Physiol **26:** 625–639

Andersson B, Anderson JM (1980) Lateral heterogeneity in the distribution of chlorophyll-protein complexes of the thylakoid membranes of spinach chloroplasts. Biochim Biophys Acta **593:** 427–440

Andreasson E, Albertsson P (1993) Heterogeneity in Photosystem I - the larger antenna of Photosystem Ia is due to functional connection to a special pool of LHCII. Biochim Biophys Acta **1141:** 175–182

Ballottari M, Govoni C, Caffarri S, Morosinotto T (2004) Stoichiometry of LHCI antenna polypeptides and characterization of gap and linker pigments in higher plants Photosystem I. Eur J Biochem **271:** 4659–4665

Barbato R, Bergo E, Szabo I, Dalla Vecchia F, Giacometti GM (2000) Ultraviolet B exposure of whole leaves of barley affects structure and functional organization of photosystem II. J Biol Chem **275:** 10976–10982

Bassi R, Giacometti GM, Simpson DJ (1988) Changes in the organization of stroma membranes induced by in vivo State-1-State-2 transition. Biochim Biophys Acta **935:** 152–165

Bassi R, Simpson D (1987) Chlorophyll-protein complexes of barley photosystem-I. Eur J Biochem **163:** 221–230

Bell AJ, Frankel LK, Bricker TM (2015) High yield non-detergent isolation of Photosystem I-Lightharvesting chlorophyll II membranes from spinach thylakoids: implications for the organization of the PS I antennae in higher plants. J Biol Chem **290:** 18429–18437

Bellafiore S, Bameche F, Peltier G, Rochaix JD (2005) State transitions and light adaptation require chloroplast thylakoid protein kinase STN7. Nature **433:** 892–895

Ben-Shem A, Frolow F, Nelson N (2003) Crystal structure of plant photosystem I. Nature **426:** 630–635

Benson SL, Maheswaran P, Ware MA, Hunter CN, Horton P, Jansson S, Ruban AV, Johnson MP (2015) An intact light harvesting complex I antenna system is required for complete state transitions in Arabidopsis. Nat Plants **15176**

Berthold DA, Babcock GT, Yocum CF (1981) A highly resolved, oxygen-evolving photosystem-II preparation from spinach thylakoid membranes - electron-paramagnetic-res and electron-transport properties. FEBS Lett **134:** 231–234

Blankenship RE (2014) Molecular Mechanisms of Photosynthesis. Wiley Blackwell, Hoboken, NJ

Bos I, Bland KM, Tian LJ, Croce R, Frankel LK, van Amerongen H, Bricker TM, Wientjes E (2017) Multiple LHCII antennae can transfer energy efficiently to a single Photosystem I. Biochim Biophys Acta **1858:** 371–378

Bos P, Oosterwijk A, Koehorst R, Bader A, Philippi J, van Amerongen H, Wientjes E (2019) Digitonin-sensitive LHCII enlarges the antenna of Photosystem I in stroma lamellae of Arabidopsis thaliana after far-red and blue-light treatment. Biochim Biophys Acta **1860:** 651–658

Bressan M, Bassi R, Dall'Osto L (2018) Loss of LHCI system affects LHCII re-distribution between thylakoid domains upon state transitions. Photosynth Res **135:** 251–261

Bressan M, Dall'Osto L, Bargigia I, Alcocer MJP, Viola D, Cerullo G, D'Andrea C, Bassi R, Ballottari M (2016) LHCII can substitute for LHCI as an antenna for photosystem I but with reduced light-harvesting capacity. Nat Plants **2:** 16131

Broess K, Trinkunas G, van der Weij-de Wit CD, Dekker JP, van Hoek A, van Amerongen H (2006) Excitation energy transfer and charge separation in Photosystem II membranes revisited. Biophys J **91:** 3776–3786

Castelletti S, Morosinotto T, Robert B, Caffarri S, Bassi R, Croce R (2003) Recombinant Lhca2 and Lhca3 subunits of the photosystem I antenna system. Biochemistry **42:** 4226–4234

Chukhutsina VU, Liu X, Xu P, Croce R (2020) Light-harvesting complex II is an antenna of photosystem I in dark-adapted plants. Nat Plants **6**: 860–868

Coombe DE (1957) The spectral composition of shade light in woodlands. J Ecol **45**: 823–830

Crepin A, Caffarri S (2015) The specific localizations of phosphorylated Lhcb1 and Lhcb2 isoforms reveal the role of Lhcb2 in the formation of the PSI-LHCII supercomplex in Arabidopsis during state transitions. Biochim Biophys Acta **1847**: 1539–1548

Croce R, Canino G, Ros F, Bassi R (2002) Chromophore organization in the higher-plant Photosystem II antenna protein CP26. Biochemistry **41**: 7334–7343

Croce R, Dorra D, Holzwarth AR, Jennings RC (2000) Fluorescence decay and spectral evolution in intact Photosystem I of higher plants. Biochemistry **39**: 6341–6348

Croce R, Morosinotto T, Castelletti S, Breton J, Bassi R (2002) The Lhca antenna complexes of higher plants photosystem I. Biochim Biophys Acta **1556**: 29–40

Croce R, van Amerongen H (2014) Natural strategies for photosynthetic light harvesting. Nat Chem Biol **10**: 492–501

Croce R, van Amerongen H (2020) Light harvesting in oxygenic photosynthesis: structural biology meets spectroscopy. Science **369**: eaay2058

Dekker JP, Boekema EJ (2005) Supramolecular organization of thylakoid membrane proteins in green plants. Biochim Biophys Acta **1706**: 12–39

Frenkel M, Bellafiore S, Rochaix JD, Jansson S (2007) Hierarchy amongst photosynthetic acclimation responses for plant fitness. Physiol Plant **129**: 455–459

Galka P, Santabarbara S, Khuong TT, Degand H, Morsomme P, Jennings RC, Boekema EJ, Caffarri S (2012) Functional analyses of the plant Photosystem I-Light-Harvesting Complex II supercomplex reveal that light-harvesting complex II loosely bound to Photosystem II is a very efficient antenna for Photosystem I in state II. Plant Cell **24**: 2963–2978

Goldschmidt-Clermont M, Bassi R (2015) Sharing light between two photosystems: mechanism of state transitions. Curr Opin Plant Biol **25**: 71–78

Grieco M, Suorsa M, Jajoo A, Tikkanen M, Aro EM (2015) Light-harvesting II antenna trimers connect energetically the entire photosynthetic machinery - including both photosystems II and I. Biochim Biophys Acta **1847**: 607–619

Havaux M, Dall'Osto L, Bassi R (2007) Zeaxanthin has enhanced antioxidant capacity with respect to all other xanthophylls in Arabidopsis leaves and functions independent of binding to PSII antennae(1[C][W]). Plant Physiol **145**: 1506–1520

Hogewoning SW, Wientjes E, Douwstra P, Trouwborst G, van Ieperen W, Croce R, Harbinson J (2012) Photosynthetic quantum yield dynamics: from photosystems to leaves. Plant Cell **24**: 1921–1935

Ihalainen JA, Klimmek F, Ganeteg U, van Stokkum IHM, van Grondelle R, Jansson S, Dekker JP (2005) Excitation energy trapping in photosystem I complexes depleted in Lhca1 and Lhca4. FEBS Lett **579**: 4787–4791

Jansson S (1999) A guide to the Lhc genes and their relatives in Arabidopsis. Trends Plant Sci **4**: 236–240

Jansson S, Stefansson H, Nystrom U, Gustafsson P, Albertsson PA (1997) Antenna protein composition of PS I and PS II in thylakoid sub-domains. Biochim Biophys Acta **1320**: 297–309

Jarvi S, Suorsa M, Paakkarinen V, Aro EM (2011) Optimized native gel systems for separation of thylakoid protein complexes: novel super- and mega-complexes. Biochem J **439**: 207–214

Jennings RC, Zucchelli G, Croce R, Garlaschi FM (2003) The photochemical trapping rate from red spectral states in PSI-LHCI is determined by thermal activation of energy transfer to bulk chlorophylls. Biochim Biophys Acta **1557**: 91–98

Johnson MP, Wientjes E (2020) The relevance of dynamic thylakoid organisation to photosynthetic regulation. Biochim Biophys Acta **1861**: 148039

Knoetzel J, Svendsen I, Simpson DJ (1992) Identification of the Photosystem-I antenna polypeptides in barley – isolation of 3 pigment-binding antenna complexes. Eur J Biochem **206**: 209–215

Koskela MM, Brunje A, Ivanauskaite A, Grabsztunowicz M, Lassowskat I, Neumann U, Dinh TV, Sindlinger J, Schwarzer D, Wirtz M, et al. (2018) Chloroplast acetyltransferase NSI is required for state transitions in Arabidopsis thaliana. Plant Cell **30**: 1695–1709

Kouril R, Arteni AA, Lax J, Yeremenko N, D'Haene S, Rogner M, Matthijs HCP, Dekker JP, Boekema EJ (2005) Structure and functional role of supercomplexes of IsiA and Photosystem I in cyanobacterial photosynthesis. FEBS Lett **579**: 3253–3257

Laemmli UK (1970) Cleavage of structural proteins during assembly of head of Bacteriophage-T4. Nature **227**: 680–685

Le Quiniou C, van Oort B, Drop B, van Stokkum IHM, Croce R (2015) The high efficiency of Photosystem I in the green alga *Chlamydomonas reinhardtii* is maintained after the antenna size is substantially increased by the association of light-harvesting complexes II. J Biol Chem **290**: 30587–30595

Liu Z, Yan H, Wang K, Kuang T, Zhang J, Gui L, An X, Chang W (2004) Crystal structure of spinach major light-harvesting complex at 2.72 A resolution. Nature **428**: 287–292

Longoni P, Douchi D, Cariti F, Fucile G, Goldschmidt-Clermont M (2015) Phosphorylation of the light-harvesting complex II isoform Lhcb2 is central to state transitions. Plant Physiol **169**: 2874–2883

Lunde C, Jensen PE, Haldrup A, Knoetzel J, Scheller HV (2000) The PSI-H subunit of photosystem I is essential for state transitions in plant photosynthesis. Nature **408**: 613–615

Miloslavina Y, Wehner A, Lambrev PH, Wientjes E, Reus M, Garab G, Croce R, Holzwarth AR (2008) Far-red fluorescence: A direct spectroscopic marker for LHCII oligomer formation in non-photochemical quenching. FEBS Lett **582**: 3625–3631

Mullen KM, van Stokkum IHM (2007) TIMP: An R package for modeling multi-way spectroscopic measurements. J Stat Softw **18**: 1–46

Natali A, Gruber JM, Dietzel L, Stuart MCA, van Grondelle R, Croce R (2016) Light-harvesting complexes (LHCs) cluster spontaneously in membrane environment leading to shortening of their excited state lifetimes. J Biol Chem **291**: 16730–16739

Pan XW, Ma J, Su XD, Cao P, Chang WR, Liu ZF, Zhang XZ, Li M (2018) Structure of the maize photosystem I supercomplex with light-harvesting complexes I and II. Science **360**: 1109–1112

Pribil M, Pesaresi P, Hertle A, Barbato R, Leister D (2010) Role of plastid protein phosphatase TAP38 in LHCII dephosphorylation and thylakoid electron flow. PLoS Biol **8**: E1000288

Qin XC, Suga M, Kuang TY, Shen JR (2015) Structural basis for energy transfer pathways in the plant PSI-LHCI supercomplex. Science **348**: 989–995

Rochaix JD (2014) Regulation and dynamics of the light-harvesting system. Annu Rev Plant Biol **65**: 287–309

Russo M, Petropoulos V, Molotokaite E, Cerullo G, Casazza AP, Maiuri M, Santabarbara S (2020) Ultrafast excited-state dynamics in land plants Photosystem I core and whole supercomplex under oxidised electron donor conditions. Photosynth Res **144**: 221–233

Santabarbara S, Tibiletti T, Remelli W, Caffarri S (2017) Kinetics and heterogeneity of energy transfer from light harvesting complex II to photosystem I in the supercomplex isolated from Arabidopsis. Phys Chem Chem Phys **19**: 9210–9222

Sauer K, Smith JRL, Schultz AJ (1966) Dimerization of chlorophyll a chlorophyll b and bacteriochlorophyll in solution. J Am Chem Soc **88**: 2681

Schmid VHR, Cammarata KV, Bruns BU, Schmidt GW (1997) In vitro reconstitution of the photosystem I light-harvesting complex LHCI-730: heterodimerization is required for antenna pigment organization. Proc Natl Acad Sci USA **94**: 7667–7672

Shapiguzov A, Ingelsson B, Samol I, Andres C, Kessler F, Rochaix JD, Vener AV, Goldschmidt-Clermont M (2010) The PPH1 phosphatase is specifically involved in LHCII dephosphorylation and

state transitions in Arabidopsis. Proc Natl Acad Sci USA **107:** 4782–4787

Slavov C, Ballottari M, Morosinotto T, Bassi R, Holzwarth AR (2008) Trap-limited charge separation kinetics in higher plant photosystem I complexes. Biophys J **94:** 3601–3612

Snellenburg JJ, Laptenok SP, Seger R, Mullen KM, van Stokkum IHM (2012) Glotaran: a Java-based graphical user interface for the R package TIMP. J Stat Softw **49:** 1–22

Spitschan M, Aguirre GK, Brainard DH, Sweeney AM (2016) Variation of outdoor illumination as a function of solar elevation and light pollution. Sci Rep **6:** 26756

Taylor CR, van Ieperen W, Harbinson J (2019) Demonstration of a relationship between state transitions and photosynthetic efficiency in a higher plant. Biochem J **476:** 3295–3312

Tikkanen M, Grieco M, Kangasjarvi S, Aro EM (2010) Thylakoid protein phosphorylation in higher plant chloroplasts optimizes electron transfer under fluctuating light. Plant Physiol **152:** 723–735

Tikkanen M, Nurmi M, Suorsa M, Danielsson R, Mamedov F, Styring S, Aro EM (2008) Phosphorylation-dependent regulation of excitation energy distribution between the two photosystems in higher plants. Biochim Biophys Acta **1777:** 425–432

van Grondelle R, Gobets B (2004) Transfer and trapping of excitations in plant photosystems. *In* Govindjee, GC Papageorgiou, eds, Chlorophyll a Fluorescence: A Signature of Photosynthesis. Advances in Photosynthesis and Respiration, Vol **19**. Springer, Dordrecht, pp 107–132

van Oort B, Alberts M, de Bianchi S, Dall'Osto L, Bassi R, Trinkunas G, Croce R, van Amerongen H (2010) Effect of antenna-depletion in photosystem II on excitation energy transfer in Arabidopsis thaliana. Biophys J **98:** 922–931

van Oort B, Amunts A, Borst JW, van Hoek A, Nelson N, van Amerongen H, Croce R (2008) Picosecond fluorescence of intact and dissolved PSI-LHCI crystals. Biophys J **95:** 5851–5861

van Oort B, Murali S, Wientjes E, Koehorst RBM, Spruijt RB, van Hoek A, Croce R, van Amerongen H (2009) Ultrafast resonance energy transfer from a site-specifically attached fluorescent chromophore reveals the folding of the N-terminal domain of CP29. Chem Phys **357:** 113–119

van Stokkum IHM, van Oort B, van Mourik F, Gobets B, van Amerongen H (2008) (Sub)-picosecond spectral evolution of fluorescence studied with a synchroscan streak-camera system and target analysis. *In* Matysik J, Aartsma, TJ, eds, Biophysical Techniques in Photosynthesis II, Springer, Dordrecht, The Netherlands, pp 223–240

Wientjes E, Croce R (2011) The light-harvesting complexes of higher-plant Photosystem I: Lhca1/4 and Lhca2/3 form two red-emitting heterodimers. Biochem J **433:** 477–485

Wientjes E, Oostergetel GT, Jansson S, Boekema EJ, Croce R (2009) The role of Lhca complexes in the supramolecular organization of higher plant Photosystem I. J Biol Chem **284:** 7803–7810

Wientjes E, van Amerongen H, Croce R (2013) LHCII is an antenna of both photosystems after long-term acclimation. Biochim Biophys Acta **1827:** 420–426

Wientjes E, van Stokkum IHM, van Amerongen H, Croce R (2011) Excitation-energy transfer dynamics of higher plant photosystem I light-harvesting complexes. Biophys J **100:** 1372–1380

Wientjes E, van Stokkum IHM, van Amerongen H, Croce R (2011) The role of the individual Lhcas in Photosystem I excitation energy trapping. Biophys J **101:** 745–754

Wood WHJ, Barnett SFH, Flannery S, Hunter CN, Johnson MP (2019) Dynamic thylakoid stacking is regulated by LHCII phosphorylation but not its interaction with PSI. Plant Physiol **180:** 2152–2166

Zhang SP, Scheller HV (2004) Light-harvesting complex II binds to several small subunits of Photosystem I. J Biol Chem **279:** 3180–3187